Electronic Supplementary Material (ESI) for ChemComm.

Supporting Information

Highly Reversible Li Metal Anode Using a Binary Alloy Interface

Jiahe Chen‡[a,b], Zejun Sun‡[a], Zhendong Li[a], Jun Liu*[,b], Xiayin Yao*[,a], Zhe Peng*[,a]

[a]Ningbo Institute of Materials Technology and Engineering, Chinese Academy of Sciences, Ningbo, 315201, China.

[b]Guangdong Provincial Key Laboratory of Advanced Energy Storage Materials, School of Materials Science and Engineering, South China University of Technology, Guangzhou, 510641, China.

‡These authors contributed equally to this work.

To whom correspondence should be addressed: msjliu@scut.edu.cn; yaoxy@nimte.ac.cn; pengzhe@nimte.ac.cn

Experimental Section

Electrode preparations: Silver bis(trifluoromethanesulfonyl)imide (AgTFSI), antimony trifluoride (SbF_3) and ethylene glycol dimethyl ether (DME) were purchased from Aladdin. Zinc bis(trifluoromethanesulfonyl)imide ($Zn(TFSI)_2$) was purchased from Energy Chemical Corporation. Battery grade Lithium bis(trifluoromethanesulphonyl)imide (LiTFSI), ethylene carbonate (EC), diethyl carbonate (DEC) and fluoroethylene carbonate (FEC) were purchased from Sigma-Aldrich Co, LLC and used as received. To prepare the Ag^+ precursor solution, 0.1 mol L^{-1} (M) AgTFSI was dissolve in DME solution and stored in an Ar filled glove box in dark environment. The Li-Ag electrodes were fabricated by simple replacement reaction in the above-mentioned glove box. 100 μL AgTFSI-DME precursor solution was evenly dropped on the surface of Li foil (thickness: 50 μm, diameter: 16 mm, China Energy Lithium Co., Ltd). After evaporation of the residual DME solution, a dark surface consisting of Ag nanostructures was obtained on the Li surface, corresponding to the Li-Ag electrode. The Li-Ag-Zn electrodes were fabricated by *in-situ* electro-reduction of Zn^{2+} on the Li-Ag electrodes. A baseline electrolyte consists of 1.0 M LiTFSI in EC:DEC (1:1 by vol.) with 5 vol% FEC was prepared first, then the selected amount of $Zn(TFSI)_2$ was added into the baseline electrolyte to prepare the Zn^{2+} containing electrolyte. The Li-Ag-Zn electrode can be *in-situ* formed during the cycling of the battery using the Zn^{2+} containing electrolyte. By replacing the Ag^+ precursor solution by a Sb^{3+} precursor solution (0.1 M SbF_3 in DME), the Li-Sb and Li-Sb-Zn electrodes were prepared by the same ways as for the Li-Ag and Li-Ag-Zn electrodes.

Electrochemical tests: CR2032 coin cells were used for cell assembly, and Celgard separators containing 70 μL electrolyte were placed in the cells. Galvanostatic deposition/stripping experiments were conducted on the symmetric cells. Thick $LiFePO_4$ cathodes with a high areal capacity of 2.5 mAh cm^{-2} were adopted to fabricate the Li || $LiFePO_4$ full cells. All the full cells were pre-cycled for five cycles at charge/discharge rates of 0.1C/0.1C in the voltage window of 2.5-4.4 V vs. Li/Li^+, followed by cycling at 0.5C/0.5C. All the electrochemical cycling test were performed on a LAND system (CT2001A) at 30 ^oC.

Materials characterization: The crystalline phase was probed by XRD with a Bruker D8 ADVANCE diffractometer using Cu Kα radiation (1.5406 Å). Before XRD characterization, the electrodes were wrapped by polyimide film to avoid the contact with ambient environment. The surface chemistry of the samples was analyzed by a PHI 3056 XPS system using a Mg Kα radiation excited source with a constant power of 100 W (15 kV and 6.67 mA). The morphology of the samples was studied by a scanning electron microscope of FEI QUANTA 250 FEG. Ionic conductivities were measured by using a DDS-307A conductivity meter (LEICI, Shanghai INESA Co.) in a glovebox (MBRAUN, $H_2O \leqslant 0.1$ ppm, $O_2 \leqslant 0.1$ ppm).

Tab. S1 Li diffusion coefficient in different alloys.

Alloy	Li diffusion coefficient (cm^2 s^{-1})	Reference
Li (self-diffusion)	5.7×10^{-11}	[1]
Li-Zn alloy	4.0×10^{-7}	[2]
Li-Ag alloy	2.4×10^{-9}	[3]
Li-Al alloy	6.0×10^{-10}	[4]
Li-Mg alloy	2.5×10^{-8}	[5]

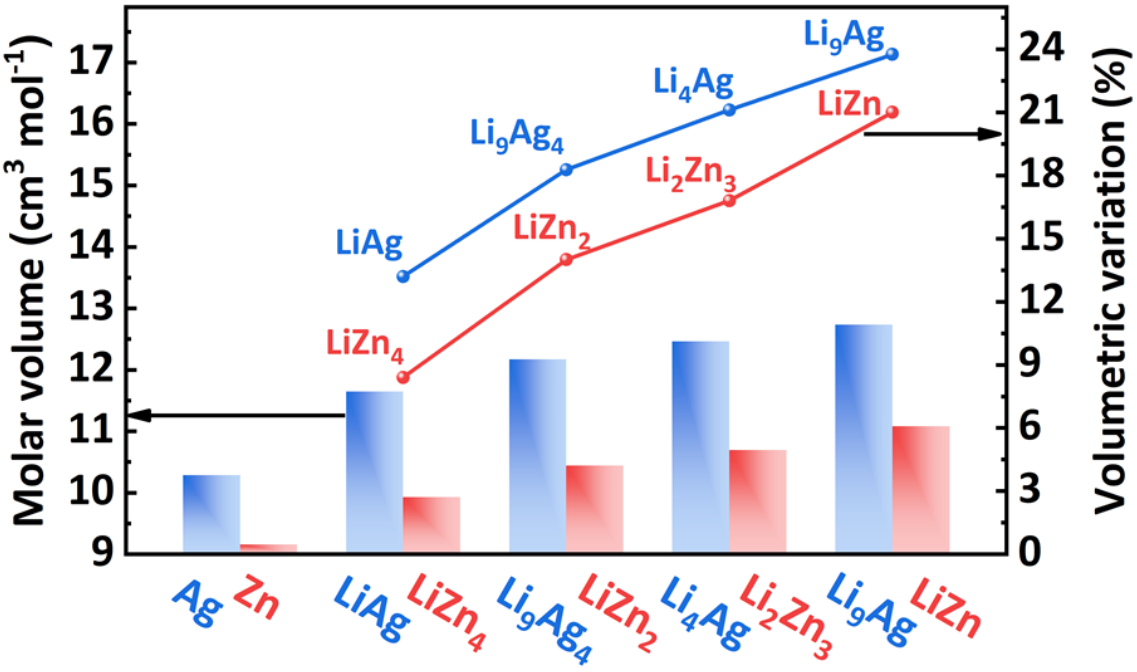

Fig. S1 Comparison of molar volume and volumetric variation of different Li-Ag and Li-Zn alloys.

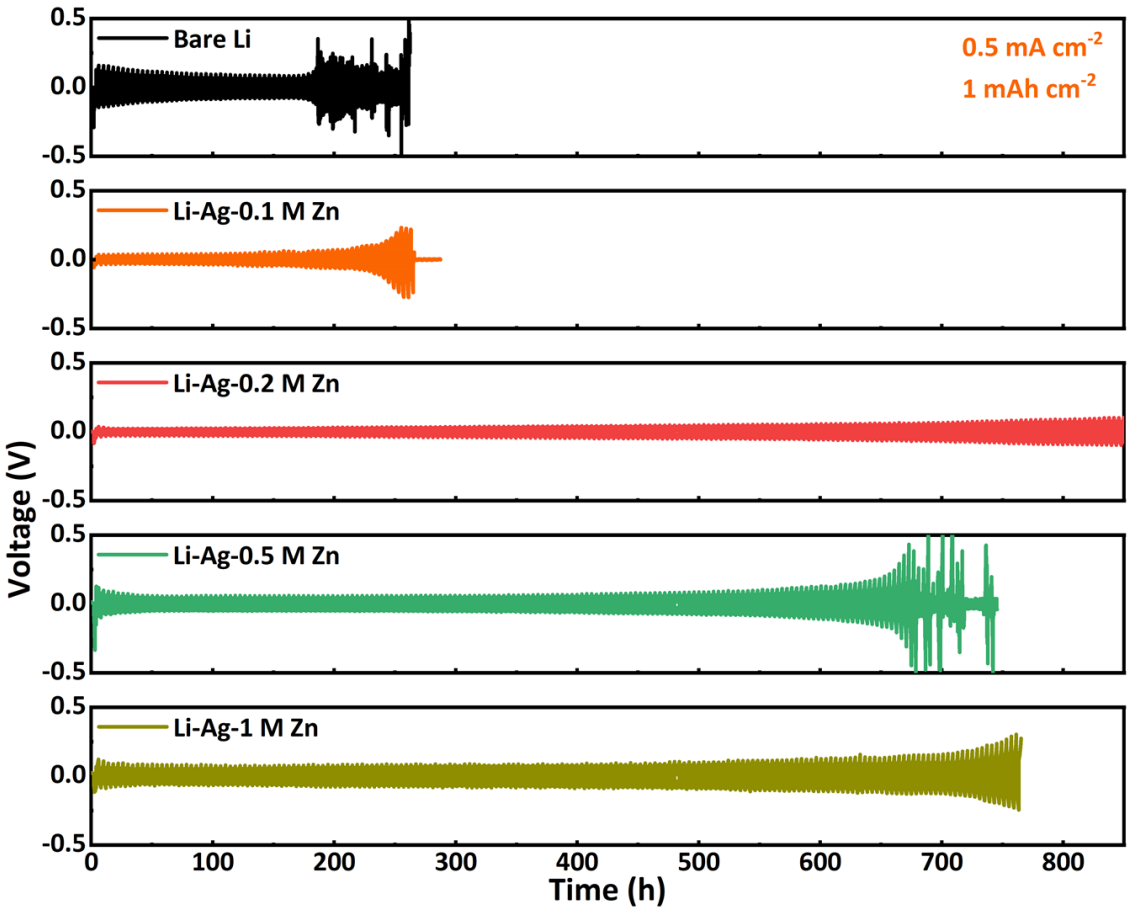

Fig. S2 Time-voltage profiles of symmetric cells using bare Li or Li-Ag-Zn electrodes under 0.5 mA cm^{-2} and 1 mAh cm^{-2}. Herein, the impact of $Zn(TFSI)_2$ amount in the electrolyte on the performances of Li-Ag-Zn electrodes is investigated systematically, where the sample notation of Li-Ag-x M Zn depicts x M $Zn(TFSI)_2$ added in the baseline electrolyte to form the Li-Ag-Zn electrodes upon cycling.

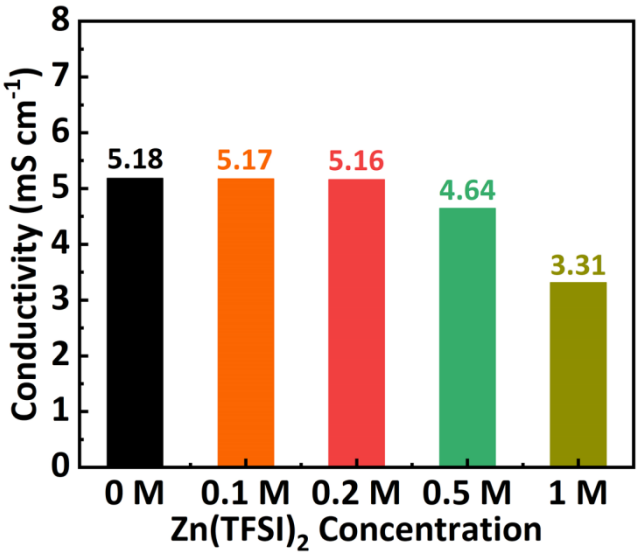

Fig. S3 Ionic conductivities of the baseline electrolyte with various $Zn(TFSI)_2$ concentrations.

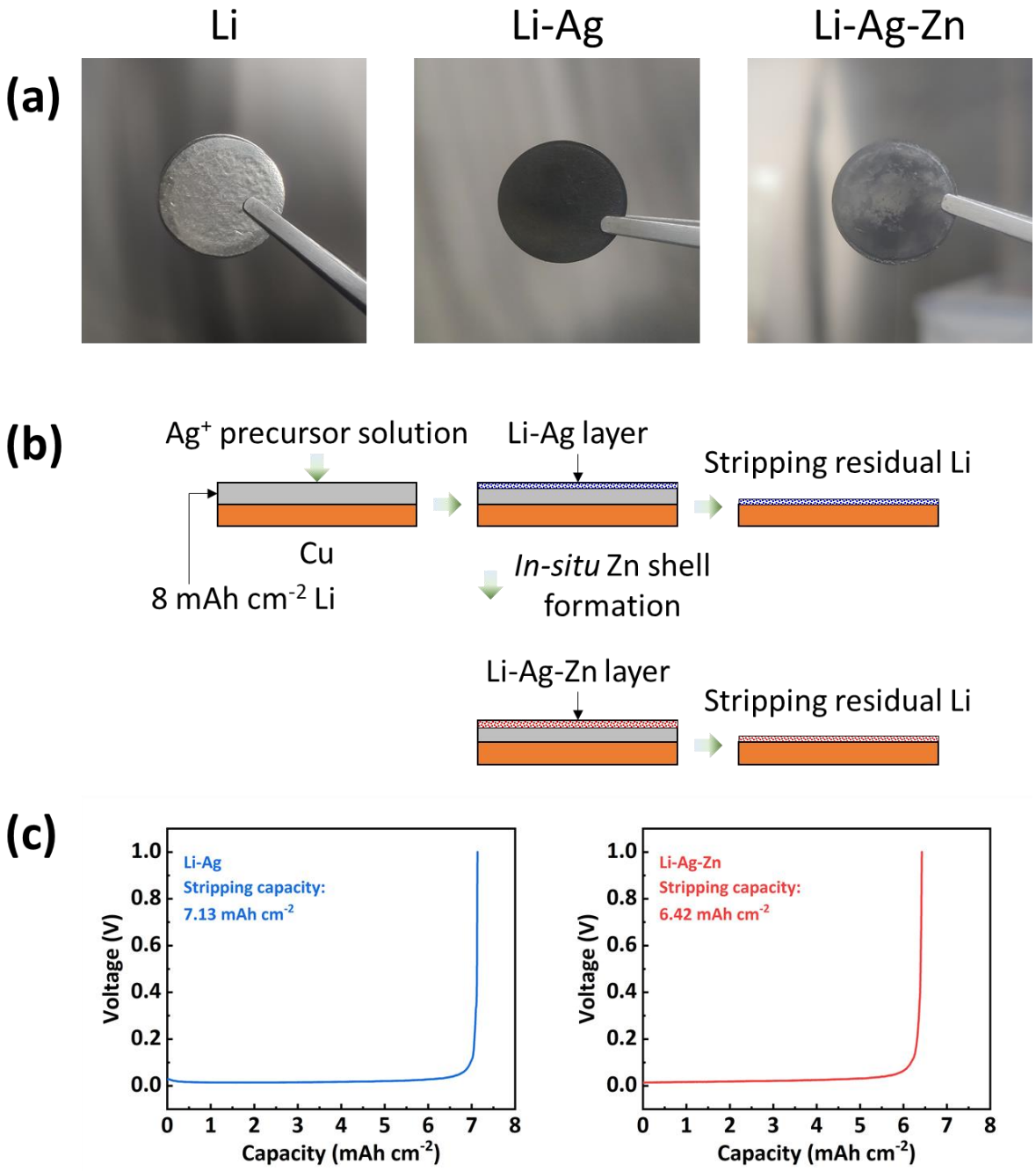

Fig. S4 (a) Photograph of Li, Li-Ag and Li-Ag-Zn. (b) Experimental process to determine the reacted Li amount during the surface modification. Briefly, an amount of 8 mAh cm^{-2} Li was electroplated on a Cu foil, on which the Ag^{+} precursor solution was dropped to form the Li-Ag layer. The Li-Ag layer coated electrode was then subjected to Li stripping process up to 1 V versus Li/Li^{+} to remove the residual Li, and the reacted Li amount during the Li-Ag

surface modification can be estimated by the difference between the stripping and initial capacities. The reacted Li amount during the Li-Ag-Zn surface modification can be estimated by the same way, except an additional process of the *in-situ* Zn shell formation (using the baseline electrolyte with 0.2 M $Zn(TFSI)_2$ and cycling under 0.5 mA cm^{-2} – 1 mAh cm^{-2} for 5 cycles prior to the Li stripping process). (c) Voltage profile of the Li stripping process of the Li-Ag or Li-Ag-Zn layer coated electrodes.

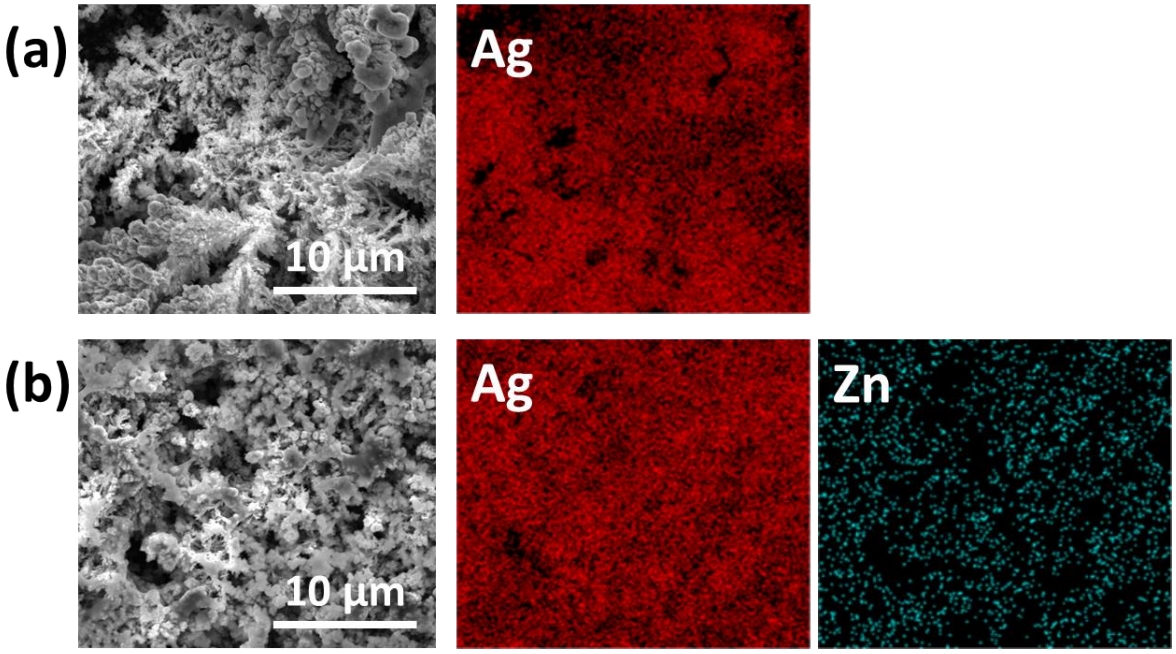

Fig. S5 SEM and EDS images of (a) Li-Ag and (b) Li-Ag-Zn electrodes.

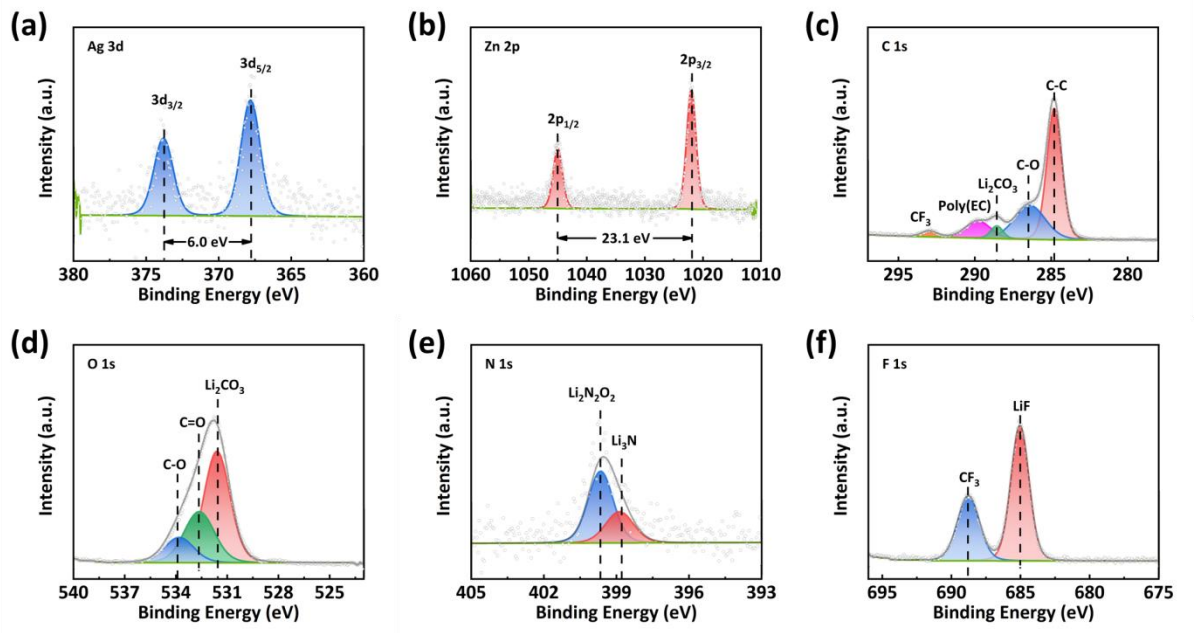

Fig. S6 (a) Ag 3d, (b) Zn 2p, (c) C1s, (d) O 1s, (e) N 1s and (f) F 1s XPS spectra of Li-Ag-Zn electrode.

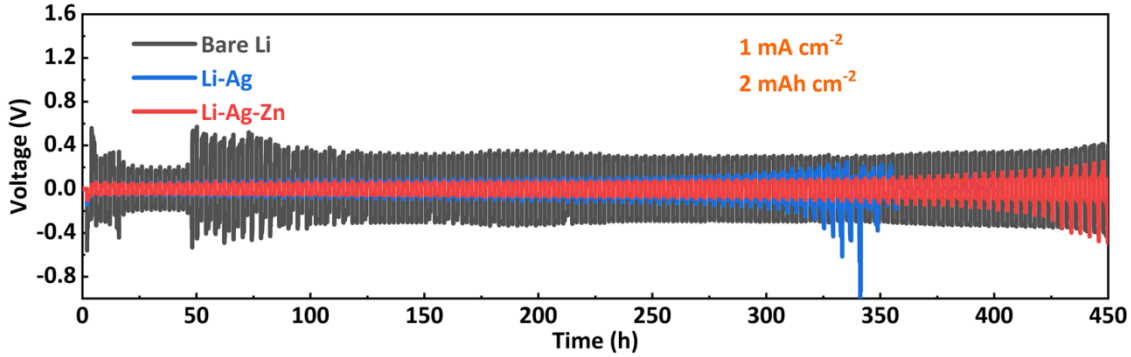

Fig. S7 Cycling performances of symmetric cells using Li, Li-Ag or Li-Ag-Zn electrodes under 1 mA cm^{-2} and 2 mAh cm^{-2}.

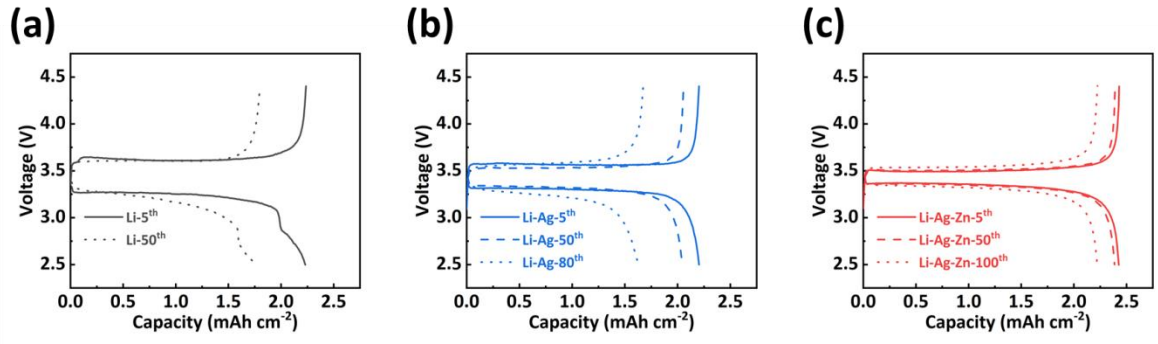

Fig. S8 Charge/discharge curves of Li || $LiFePO_4$ full cells using (a) Li, (b) Li-Ag or (c) Li-Ag-Zn electrodes.

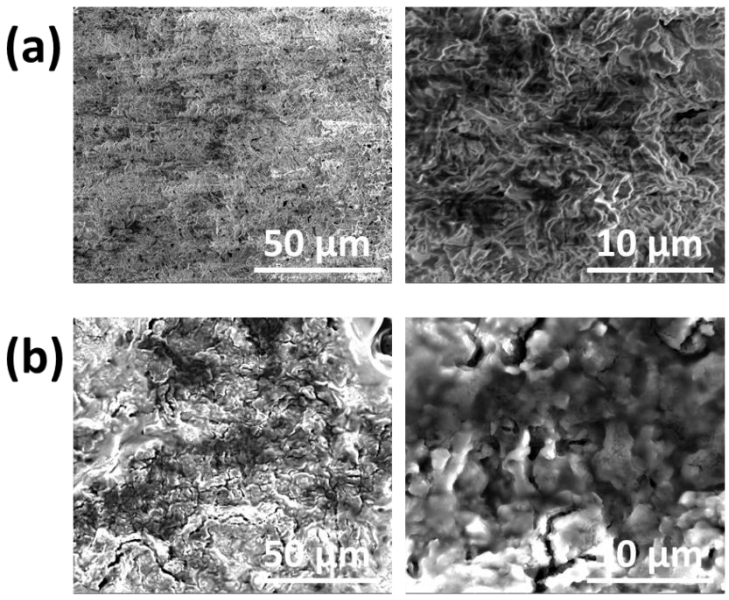

Fig. S9 SEM images of the cycled Li electrodes disassembled from the Li ‖ $LiFePO_4$ full cells after (a) 5 and (b) 50 cycles.

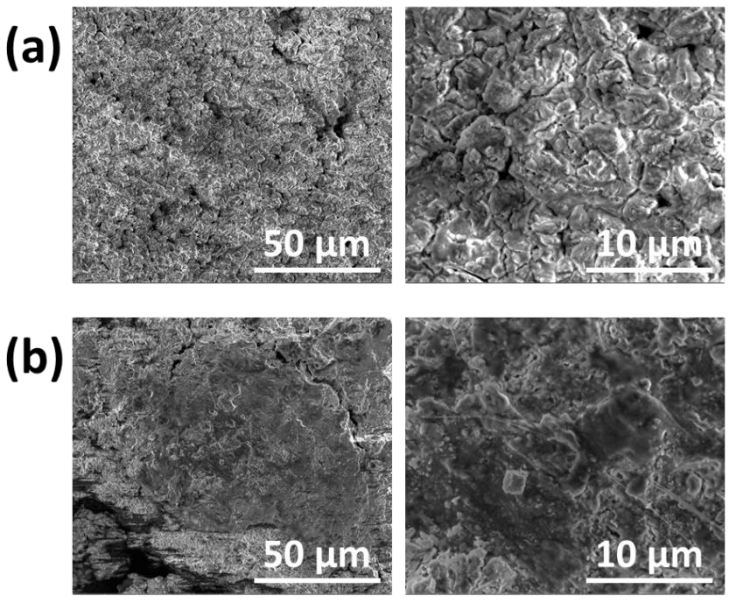

Fig. S10 SEM images of the cycled Li-Ag electrodes disassembled from the Li ‖ $LiFePO_4$ full cells after (a) 5 and (b) 50 cycles.

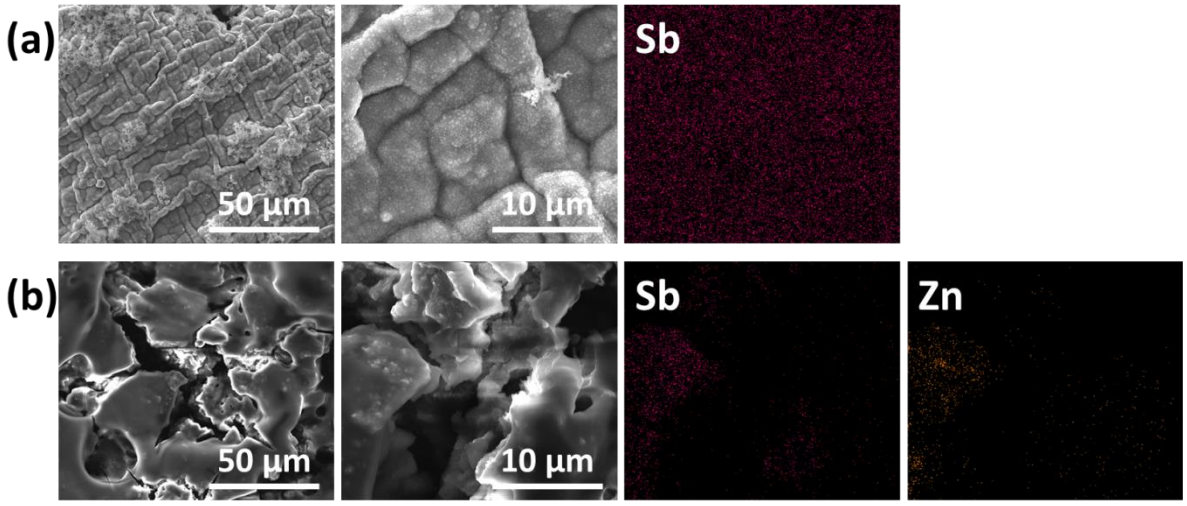

Fig. S11 SEM and EDS images of (a) Li-Sb and (b) Li-Sb-Zn electrodes.

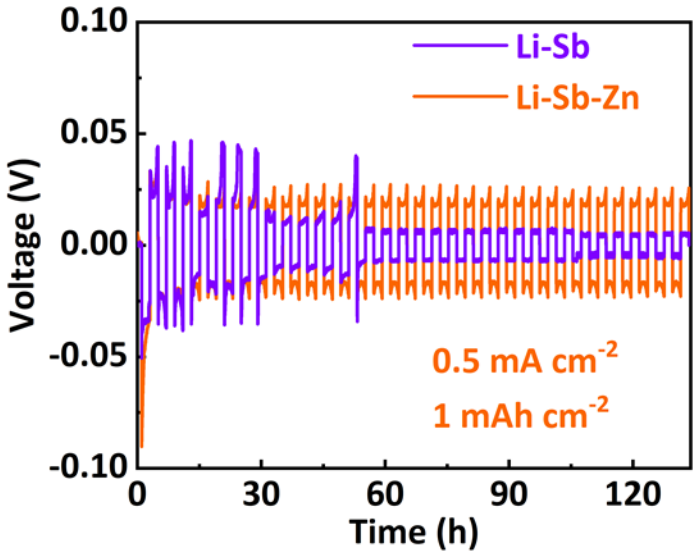

Fig. S12 Cycling performances of symmetric cells using Li-Sb or Li-Sb-Zn electrodes under 0.5 mA cm^{-2} and 1 mAh cm^{-2}.

References

1. E. Dologlou, *Glass Phys. Chem.*, 2010, **36,** 570-574.

2. A. Hu, W. Chen, X. Du, Y. Hu, T. Lei, H. Wang, L. Xue, Y. Li, H. Sun, Y. Yan, J. Long, C. Shu, J. Zhu, B. Li, X. Wang and J. Xiong, *Energy Environ. Sci.*, 2021, **14,** 4115-4124.

3. S. Jin, Y. Ye, Y. Niu, Y. Xu, H. Jin, J. Wang, Z. Sun, A. Cao, X. Wu, Y. Luo, H. Ji and L.-J. Wan, *J. Am. Chem. Soc.*, 2020, **142,** 8818-8826.

4. S. Qu, W. Jia, Y. Wang, C. Li, Z. Yao, K. Li, Y. Liu, W. Zou, F. Zhou, Z. Wang and J. Li, *Electrochim. Acta*, 2019, **317,** 120-127.

5. Z. Shi, M. Liu, D. Naik and J. L. Gole, *J. Power Sources*, 2001, **92,** 70-80.